PNAS PLUS

Massive increase in visual range preceded the origin of terrestrial vertebrates

Malcolm A. MacIver[a,b,c,1], Lars Schmitz[d,e,1], Ugurcan Mugan[c], Todd D. Murphey[b], and Curtis D. Mobley[f]

[a]The Neuroscience and Robotics Laboratory, Northwestern University, Evanston, IL 60208; [b]Department of Mechanical Engineering, Northwestern University, Evanston, IL 60208; [c]Department of Biomedical Engineering, Northwestern University, Evanston, IL 60208; [d]W. M. Keck Science Department, Claremont McKenna, Pitzer, and Scripps Colleges, Claremont, CA 91711; [e]Dinosaur Institute, Natural History Museum of Los Angeles County, Los Angeles, CA 90007; and [f]Section for Optical Oceanography, Sequoia Scientific, Inc., Bellevue, WA 98005

Edited by Neil H. Shubin, The University of Chicago, Chicago, IL, and approved January 24, 2017 (received for review September 17, 2016)

The evolution of terrestrial vertebrates, starting around 385 million years ago, is an iconic moment in evolution that brings to mind images of fish transforming into four-legged animals. Here, we show that this radical change in body shape was preceded by an equally dramatic change in sensory abilities akin to transitioning from seeing over short distances in a dense fog to seeing over long distances on a clear day. Measurements of eye sockets and simulations of their evolution show that eyes nearly tripled in size just before vertebrates began living on land. Computational simulations of these animal's visual ecology show that for viewing objects through water, the increase in eye size provided a negligible increase in performance. However, when viewing objects through air, the increase in eye size provided a large increase in performance. The jump in eye size was, therefore, unlikely to have arisen for seeing through water and instead points to an unexpected hybrid of seeing through air while still primarily inhabiting water. Our results and several anatomical innovations arising at the same time suggest lifestyle similarity to crocodiles. The consequent combination of the increase in eye size and vision through air would have conferred a 1 million-fold increase in the amount of space within which objects could be seen. The "buena vista" hypothesis that our data suggest is that seeing opportunities from afar played a role in the subsequent evolution of fully terrestrial limbs as well as the emergence of elaborated action sequences through planning circuits in the nervous system.

fish–tetrapod transition | vision | visual ecology | terrestriality | prospective cognition

Before terrestrial vertebrates arose, their ancestors inhabited underwater environments, where vision is highly compromised compared with vision above water. The visual difference between life in water and life above it is comparable with driving fast on a foggy road, where our responses must be rapid and simple, vs. driving in clear daylight conditions, where deliberation over more complex choices is enabled by the vast increase in sensory range. Nonetheless, although an immense quantity of work has been done on the emergence of limbs during the evolution of land vertebrates, how visual capability changed during the transition from water to land has not been explored. In part, this lack of exploration is because computational visual ecology—necessary to interpret the fossil data—has not been combined with early tetrapod paleontology. Through combining these disciplines, here we probe the evolutionary history of the switch in our visual sensory ecology from water to air. Surprisingly, our results show that eyes tripled in size just before full-time life on land evolved. Convergent lines of evidence, including our own, strongly support the hypothesis that a crocodilian ecotype—using the greatly enhanced visual capabilities conferred by vision through air to prey on the bounty of unexploited invertebrates that long preceded the vertebrates onto land—was the gateway between vertebrate life underwater and on land.

Large Eyes Appeared Before Terrestriality

Fig. 1 shows the sequence of steps of our study across its parent disciplines. We start with the assembly of a time-calibrated phylogeny of 59 tetrapodomorph taxa that bracket the water–land transition and have measurable skull and eye socket lengths (*Materials and Methods*). We generated a set of 1,000 evolutionary trees to account for uncertainties in phylogeny. Using this tree distribution, we then apply a phylogenetic comparative approach to estimate whether there were changes in the selective regime governing the evolution of relative eye socket length (socket length corrected for size of animal inferred from skull length by a regression). A statistical approach incorporating phylogenetic information is needed, because the evolutionary relationships of the animals in our sample result in our observations of their eye socket sizes losing statistical independence (1, 2), disqualifying conventional significance tests that depend on this property. Specifically, we follow an approach guided by the Ornstein–Uhlenbeck (OU) process as a model of trait evolution (3, 4). We use a Bayesian variant of this method (5) to study the adaptive landscape of the relative eye socket sizes of early tetrapods (*Materials and Methods*).

Analysis of the selective regime shifts within the tree distribution reveals a surprising finding: a change favoring larger eye sockets is most likely to have happened before the origin of the vertebrates with complete limbs including fingers and toes (hereafter "digited tetrapods"), in animals understood to be primarily aquatic (Fig. 2). This major shift in eye socket evolution occurred

Significance

Starting 385 million years ago, certain fish slowly evolved into legged animals living on land. We show that eyes tripled in size and shifted from the sides to the top of the head long before fish modified their fins into limbs for land. Before permanent life on land, these animals probably hunted like crocodiles, looking at prey from just above the water line, where the vastly higher transparency of air enabled long-distance vision and selected for larger eyes. The "buena vista" hypothesis that our study forwards is that seeing opportunities far away provided an informational zip line to the bounty of invertebrate prey on land, aiding selection for limbs—first for brief forays onto land and eventually, for life there.

Author contributions: M.A.M. and L.S. designed research; M.A.M. and L.S. performed research; T.D.M. contributed new reagents/analytic tools; M.A.M., L.S., U.M., and C.D.M. analyzed data; and M.A.M. and L.S. wrote the paper.

The authors declare no conflict of interest.

This article is a PNAS Direct Submission.

Freely available online through the PNAS open access option.

Data deposition: Code and data to reproduce these results is available at https://doi.org/10.5281/zenodo.321923.

[1]To whom correspondence may be addressed. Email: maciver@northwestern.edu or lschmitz@kecksci.claremont.edu.

This article contains supporting information online at www.pnas.org/lookup/suppl/doi:10.1073/pnas.1615563114/-/DCSupplemental.

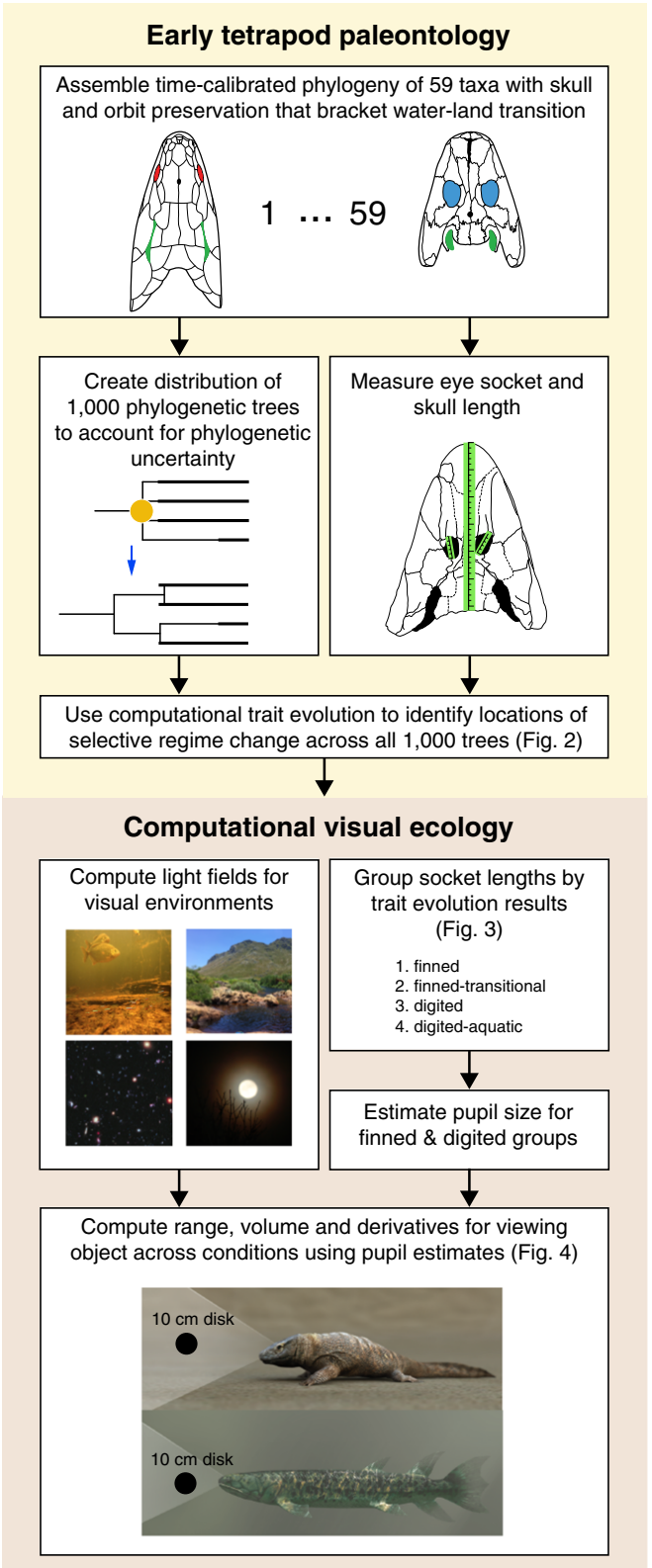

Fig. 1. The sequence of steps within early tetrapod paleontology as well as computational visual ecology used for generating the results of this study.

in a phase of fundamental reorganization of the tetrapod body plan. The transitional phase begins with the lineage leading to the last ancestor of the elpistostegalians (the finned transitional group in Fig. 2) and ends with the lineage connecting to the last ancestor of the very first digited tetrapods, *Ventastega* (inferred to have digits) and *Acanthostega*. During this phase of evolution, tetrapods entered a new adaptive zone that selected relative eye socket sizes that were a factor of 1.42–1.53 larger than the ancestral adaptive peak for fish, such as *Eusthenopteron* (Fig. 2). Fig. 3 shows the absolute and relative socket sizes for our dataset grouped according to the adaptive zones identified by the analysis of selective regime shifts. We refer to the group before the increase in eye socket size as "finned tetrapods" (6). As shown in Fig. 3, there was a near tripling in the mean absolute socket size between the finned and digited tetrapods. We will show below that the enlargement of eye sockets supports the inference that eyes also approximately tripled in size.

Interestingly, there was a reversion to small eye sockets in a group of animals that subsequently specialized for life underwater. This group is termed the "adelospondyl-colosteids" (7) (Figs. 2 and 3). They have elongated snake-like bodies with tiny limbs (7, 8) and shrunken eye sockets similar to those of the finned tetrapods. Although there are other animals that are clearly semiaquatic within the digited tetrapods, the adelospondyl-colosteids are unique in the extent of aquatic specialization across the entire group and considered fully aquatic.

Our discovery that the evolution of larger eye sockets occurred in animals that were primarily aquatic is in line with other critical conclusions of the past several decades of early tetrapod paleontology, which has found that robust limbs evolved in primarily aquatic animals (9, 10) and that fingers and toes evolved in primarily aquatic animals (11). Notably, the increase in eye size starting in the elpistostegalians coincided with a distinct change in the placement of eyes in this group. Although placed laterally in the early phase of tetrapod evolution, similar to other fish, the eyes moved into a position on the top of the head in this group (*Eusthenopteron* compared with *Tiktaalik* in Fig. 2). They are on raised "eye brows," low bony prominences on the top of the skull (12–14).

Computational Visual Ecology

The adaptive landscape analysis in Fig. 2 shows the location and magnitude of changes in relative eye socket size but is insufficient for understanding their possible bases. Larger sockets strongly correlate with larger eyes as shown by data on fish (*SI Appendix, Estimating Eye and Pupil Size in Early Tetrapods* and Fig. S4), reptiles (15), birds (16), and primates (17). Evidence spanning such a broad bracket of vertebrates shows that eye socket size in our group of ancient animals reliably captures what their eye size would have been. We can, therefore, estimate that the nearly threefold increase of absolute eye socket size (Fig. 3) corresponds to an almost threefold increase in eye size. However, what are these large eyes good for? To better understand the significance of the increase in eye size, estimates of the functional consequences of these changes across environments that bracket the most likely possibilities (computational visual ecology) (Fig. 1) can be helpful.

Larger eyes are strongly correlated with larger pupils (*SI Appendix, Estimating Eye and Pupil Size in Early Tetrapods* and Fig. S4), a key variable in estimating visual capability. We selected four measures of visual function that we calculated as a function of pupil size: the distance at which a standard object, a 10-cm black disk, could be seen; the volume of space within which that same object could be seen given an estimate of the field of view; and the gains in both range and volume for a change in eye size (the derivatives of range and volume measures with respect to eye size). These measures were computed for the mean pupil size of the finned and digited groups ±1 SD as estimated from the absolute socket lengths for these groups (*Materials and Methods* and Fig. 3*A*).

To make estimates of visual range and volume, we adapted a model of aquatic visual capability for pelagic fish from Nilsson

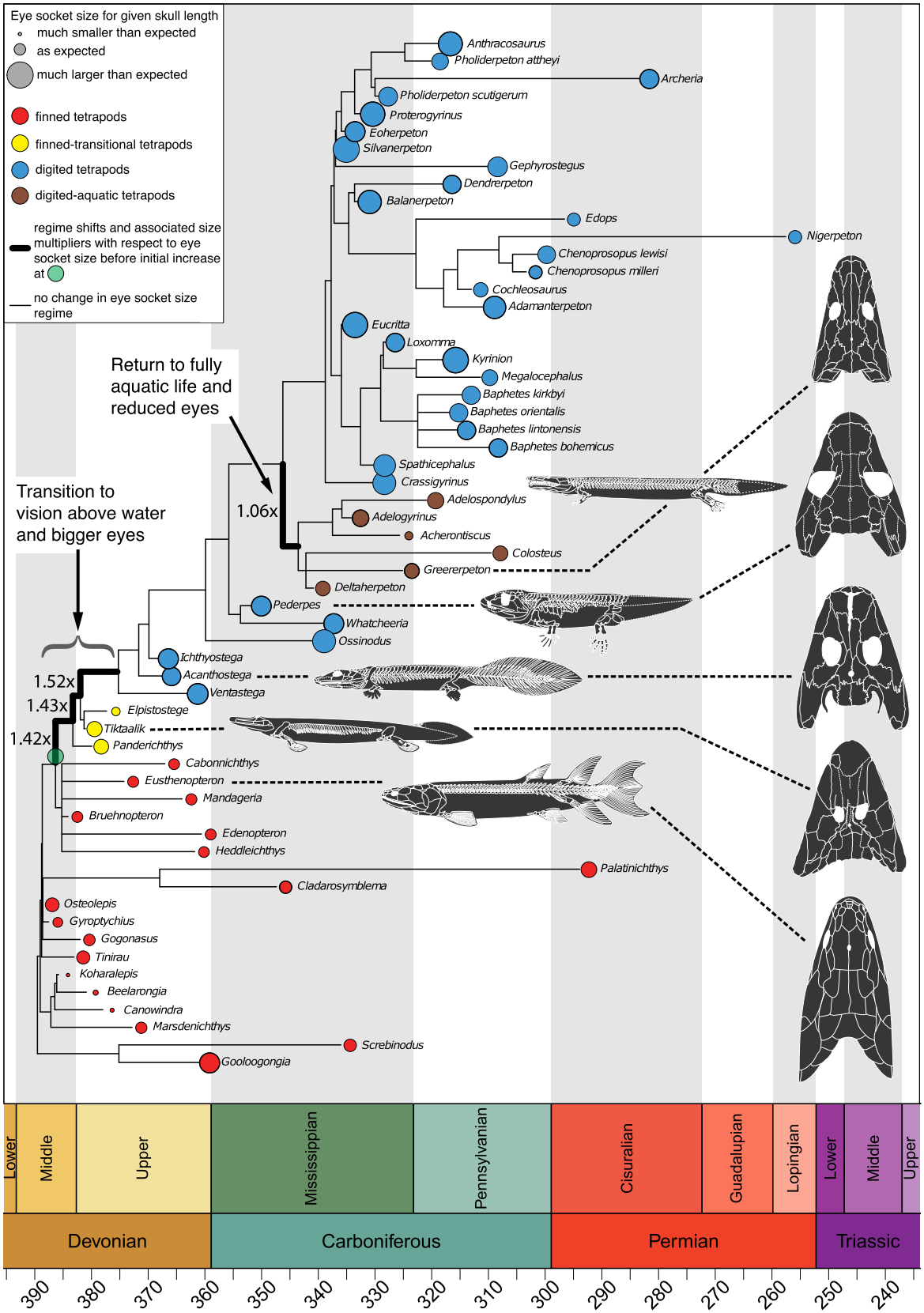

Fig. 2. Evolution and adaptive landscape of relative eye socket size in early tetrapods summarizing our phylogenetic comparative study performed over a sample of 1,000 time-calibrated trees. The circles (red for finned, yellow for finned transitional, blue for digited, and brown for digited aquatic tetrapods) represent body size-corrected relative eye socket sizes, the residuals from phylogenetically generalized least squares regression (PGLS) of $\log_{10}$-transformed variables (*Materials and Methods* and *SI Appendix, Scaling of Orbit and Skull Length in Early Tetrapods*). The thick branches indicate positions of well-supported selective regime shifts, with associated factors signifying the change in eye socket size compared with the ancestral regime (before the green dot) after body size effects are accounted for.

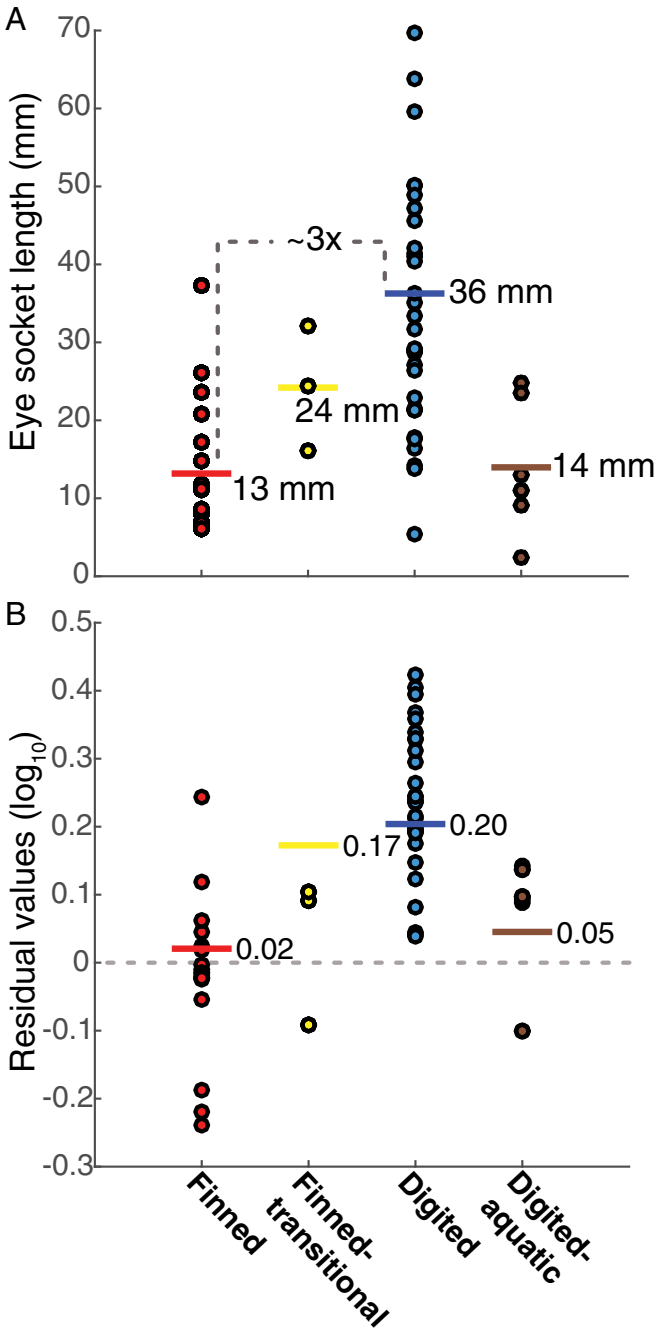

Fig. 3. Eye socket lengths across the taxa in Fig. 2 grouped by the regime shift analysis. (*A*) The mean (horizontal bars) absolute eye socket length of digited tetrapods was three times larger than that of their finned relatives, with the elpistostegalians (finned-transitional) midway. The digited tetrapods that returned to life underwater (adelospondyl-colosteids, digited-aquatic) reverted to a size similar to that of their finned relatives. (*B*) Relative eye socket size was calculated as residuals from a phylogenetically informed regression of $\log_{10}$-transformed variables (*Materials and Methods*) averaged over the full set of 1,000 trees. Positive residuals indicate eye sockets larger than expected based on skull length, whereas negative residuals indicate eye sockets smaller than expected. The Bayesian OU results in Fig. 2 show the presence of an adaptive evolutionary process and provide estimates of the adaptive peak for each group (horizontal bars). The elpistostegalians entered a new selective regime but are lagging behind, because time was insufficient to accrue enough increases in eye socket size to reach the peak. However, the digited tetrapods are centered around their adaptive peak, except for the adelospondyl-colosteids. As expected for a diverse group, not all tetrapods are at their respective peak, reflecting a normal evolutionary pattern in which trait values are dispersed around the optimal value. The Bayesian OU findings show that there must have been a selective benefit from larger eye sockets in finned transitional and digited tetrapods, but uncovering its basis requires modeling visual performance across likely environments.

et al. (18), which focused on first-order optical physics, and incorporated contrast threshold into this framework. With this change, visual ranges in aquatic and above-water environments can be calculated using the same model. The visual system is modeled with two channels: one that only sees an empty background and one that only sees a given target (18) (*Materials and Methods* and *SI Appendix, Computational Visual Sensory Ecology Estimates*). For these reasons, our visual range estimates represent a best case scenario for visual detection in the absence of clutter.

To compute the amount of light in the background and the light from the target, we must model the likely visual environments of the early tetrapods. Visual range for a given object differs greatly between aquatic and aerial environments, a fact related to their dramatically different attenuation lengths. The attenuation length of a medium is defined as $1/c$, where c is the sum of the absorption and scattering coefficients. After a beam of parallel light rays travels a distance equal to the attenuation length, a fraction of the light equal to the reciprocal of the base of the natural logarithm—≈1/2.71 or 37%—remains at the given wavelength. Aquatic attenuation lengths—for shorter wavelengths (bluish) that travel the farthest in clear water—vary in oceans from, at most, 24 m for the clearest deep water (19, 20) to meters for coastal oceanic water (18, 20) and vary in freshwater from less than 2 m to a 10th of a meter (21–23). Shallow freshwater habitats are where the majority of early tetrapods emerged (8, 9, 24–26). In dramatic contrast to the ancestral aquatic condition, the attenuation length for similar wavelengths of light in air is 25,000 m (27, 28) (extinction factor) (*SI Appendix*, Table S1)—between 10,000 and 100,000 times larger than the habitats similar to those of the early tetrapods. Additional details on the visual ecology calculations are in *Materials and Methods* and *SI Appendix*.

Our results (Fig. 4) show that visual performance underwent a massive increase with the shift from vision through water to vision through air. For the case of daytime viewing horizontally in water through finned tetrapod eyes vs. air through digited tetrapod eyes, the range increased by well over a factor of 100. A conservative estimate of the total volume that our standard object could be sensed within (*Materials and Methods*)—a more ethologically relevant measure (29, 30)—increases by just under 2 million times (Fig. 4 *A1, A2, C1*, and *C2* and *SI Appendix*, row 2 in Table S4).

We have performed a large number of sensitivity analyses to determine how robust this conclusion is to our assumptions (*Materials and Methods*, *Sensitivity Analyses*). These analyses divide into perturbations of our baseline visual environment and perturbations to our baseline visual physiology. In terms of sensitivity to environment, we note that a large increase in our measures of visual performance occurs regardless of the diel activity patterns of the early tetrapods. Our results are consequently agnostic to whether the increase in eye size was for the gain of sensitivity that this causes for the dim light vision models (leading to larger range) or because larger eyes in full light lead to an increase in acuity (also leading to larger range) (*SI Appendix, Vision Model Limitations and Sensitivity Analysis* and Table S1). Our results are also unaffected by variations in water clarity. In terms of perturbations to our baseline visual physiology, changes to a host of factors, including contrast threshold, photoreceptor size, and dark noise level among others, have effects that are well outside of the range where our conclusions are affected. For the daylight vision case, these variations are shown in Fig. 4, solid green fill.

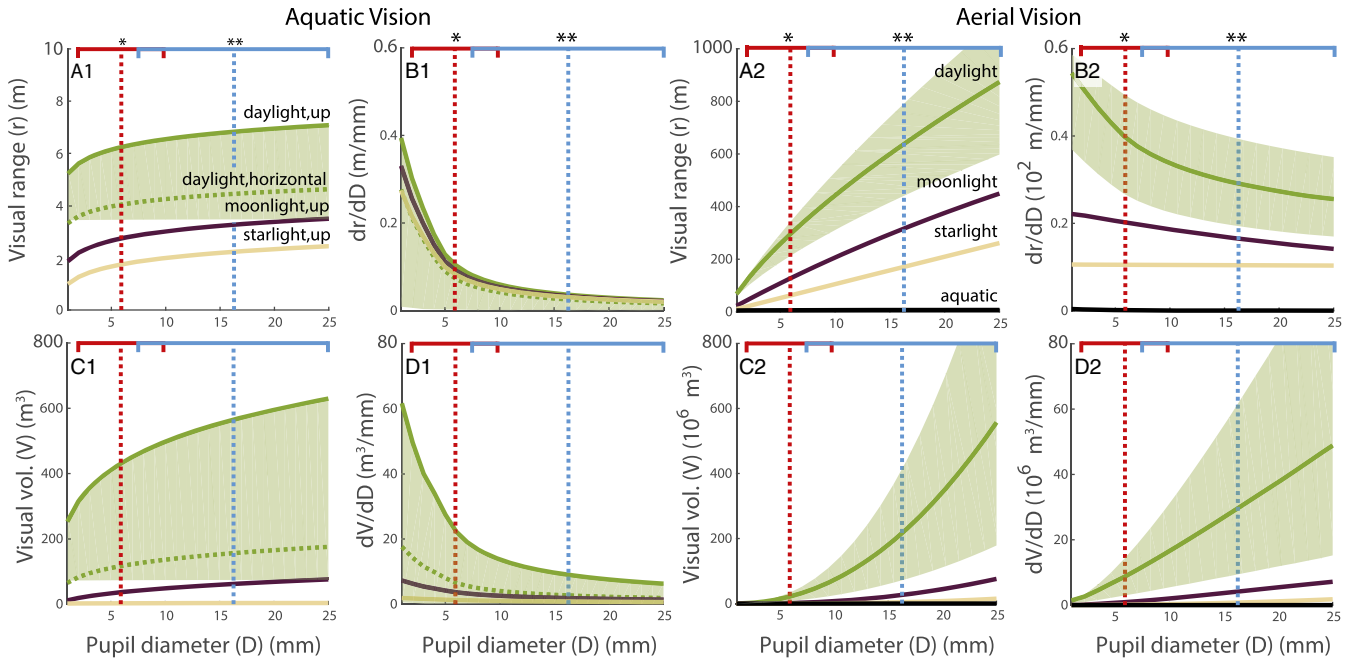

Fig. 4. Visual performance in and out of water. Aquatic vision is estimated using the Baseline River water type defined in *SI Appendix*, Table S3 at a depth of 8 m. The object is a black 10-cm-diameter disk. (*A1* and *A2*) Maximum distance that the object can be seen in water and air, respectively, under various lighting conditions. Note that visual range scales proportionately to target size. For a 1-cm disk in daylight, the aerial range decreases to 139.3 m assuming mean pupil size for digited tetrapods and 54.7 m for the mean pupil size of finned tetrapods (data not shown). (*B1* and *B2*) How much range is gained for an increase in pupil size? Note that the *y*-axis multiplier is 100 times larger in *B2*. (*C1* and *C2*) Total volume within which the standard object is visible. Note that the *y*-axis multiplier is 1 million times larger in *C2*. (*D1* and *D2*) How much volume is gained for an increase in pupil size? Note that the *y*-axis multiplier is 1 million times larger in *D2*. For the aerial plots, the aquatic values are shown but imperceptible. Uncertainty for the daylight condition (green fill) was calculated by using alternative values for the vision model (*Materials and Methods*) and is not shown for other conditions for clarity. SD is here only for showing the distribution of estimated pupil sizes; it cannot be used in this context for ascertaining significance because of shared ancestry (details are in the text). *Red horizontal bars show ±1 SD of pupil sizes from the mean (dotted vertical lines) estimated for the eye sockets of finned tetrapods. **Blue horizontal bars and vertical lines are for the digited tetrapods.

One finding that is informative given the movement of the eyes from their standard fish-like location along the sides of the head to the top (compare *Eusthenopteron* with *Tiktaalik* in Fig. 2) has to do with extended range for looking up toward the water surface vs. looking horizontally within water. Because sunlight is predominantly down-welling at shallower depths (ref. 31, figure 2.20 and ref. 32), upward viewing in these environments provides a considerable increment in range—a factor of ≈1.5 in daylight conditions (Fig. 4*A1*) at 8-m depth. At shallower depths than 8 m, this multiplicative factor increases.

Based on our results on trait evolution and computational visual ecology, we conclude that the observed increase in eye size is the result of adaptive evolution, where the derivative of the range and volume with respect to the pupil size is a proxy for the selective benefit of mutations that increase eye size. This measure shows a very clear pattern: in the transition from underwater to aerial viewing, there is a gain of ≈5 million in how much an increase in eye size increases the volume within which our standard object can be seen (Fig. 4 *D1* and *D2* and *SI Appendix*, row 2 in Table S4). In addition, for the volume derivative, there is a switch from diminishing returns for increasing pupil size (negative slope in Fig. 4*D1*) for aquatic environments to increasing returns (positive slope in Fig. 4*D2*) for the aerial case.

Discussion

Our results show that the inferred tripling of eye size achieves very little additional performance for eyes that are underwater (Fig. 4*A1*). In the most likely aquatic environments of early tetrapods, such as the lobe-finned fish *Eusthenopteron*, vision was on the order of a body length—as also estimated for contemporary coastal fish (35)—before and after the tripling of eye size. In contrast, were these eyes looking out over the waterline, a conservative estimate of the field of view gives a total visually surveyed volume increase of over 1 million times the aquatic volume (Fig. 4 *C1* vs. *C2*). Although the bulk of this increase is because of the change in environment, just examining the effect of eye size changes alone discloses that aerial performance increases a factor of 10 times more over the performance increase that happens in the aquatic case. Furthermore, for aerial vision, there is a 5 million-fold increase in the amount of space that our standard object can be seen within for a given increase in eye size compared with aquatic vision. Finally, there is a switch from diminishing returns with larger eyes in the aquatic case to increasing returns for larger eyes in the aerial case (Fig. 4 *D1* vs. *D2*).

These performance gains may explain the evolutionary increase of eye size, despite the high metabolic cost of sensory acquisition (30, 36–39), but additional insights can be gained by combining the metabolic cost of sensing with the analysis of the energetics of movement (30). This synthesis suggests that reducing the metabolic cost of predation is spread across the motor and sensory systems involved. To scan a given volume of space for prey or predators, increased energy expenditure on longer-range vision can have savings over having to translate the entire body more when sensory range is short. Similarly, swiveling a large visual sensory volume using the neck that evolved first in *Tiktaalik* is less costly than body reorientation for acquiring the same visual information (30).

The 1 million-fold gain in visually monitored space through aerial vision could, therefore, have had a favorable impact on energetics. If aerial vision and its beneficial energetics are the

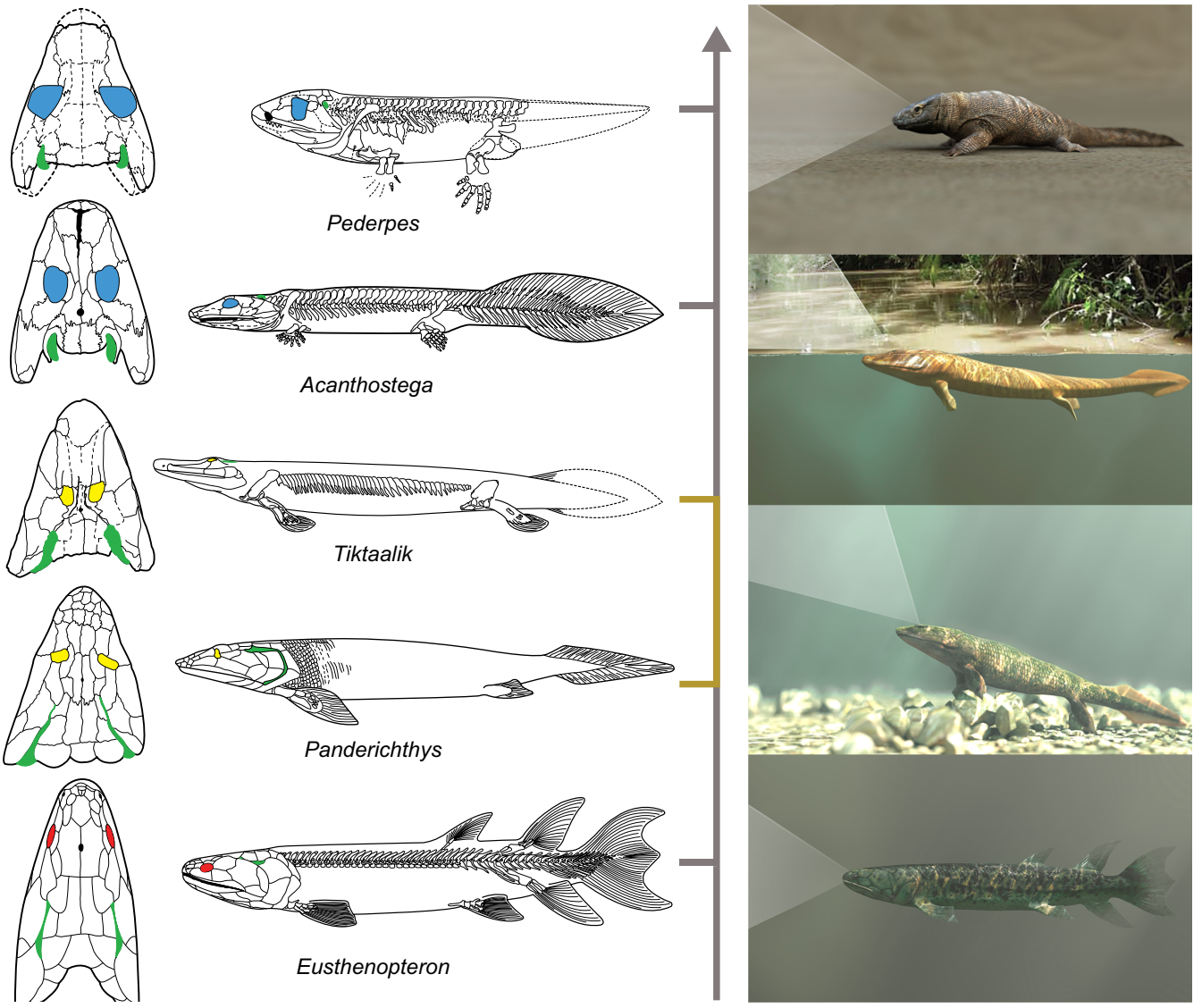

Fig. 5. A possible evolutionary scenario consistent with our results. Having invaded shallow waters, where the down-welling component of sunlight is significant, better visual range is obtained with eye sockets moved to the top of the skull, providing upward vision (Fig. 4*A1*) as shown here for *Panderichthys*. Possibly driven by low oxygen, animals surfaced near shore to breathe through the spiracles that had also dorsalized to just behind the eyes in the elpistostegalians, as shown here for *Tiktaalik*. Without correction for the differing refractive index of air, they initially saw blurry outlines of invertebrate fauna (33) that had already been living on land for 50 My. With continued surfacing and selection of the slight changes to lens and cornea to enable a focused image of their quarry, in a small fraction (34) of the 12-My transition from finned to digited tetrapod eye sizes, the full power of long-range vision would have emerged. The strong derivative of visual volume with respect to eye size would have facilitated the observed selection for larger eye size. Simultaneously, selective advantages of limbs with digits over limbs with fins made animals like *Acanthostega* better suited for longer forays onto land, culminating in more terrestrial forms, such as *Pederpes*, 30 My after *Tiktaalik*. The colored portion of the simplified tree marks an evolutionary phase with substantial body plan modifications. Shown in green in *Left* are the spiracles (what becomes the Eustachian tube) likely used for breathing at the water surface while using aerial vision. Total animal lengths are between 50 cm and 1.5 m and are not drawn to scale. Age spans from 385 My for *Eusthenopteron* to 355 My for *Pederpes*.

basis of the increase in eye size, it coincides with another change likely to improve energetics. In the transitional elpistostegalians, there is evidence for another major bodily function moving from below to above water: respiration. In this group and later taxa, there was an enlargement of breathing spiracles (also called otic notches) located behind the eyes (green in Fig. 5) (9, 13, 26, 40). The enlargement of spiracles occurred during a time of Earth's history when oxygen levels trended downward (26, 41). For aquatic animals, the Devonian decline of oxygen was exacerbated by the fact that water has 1/30th of the oxygen of air, while being 800 times denser (42, 43). Therefore, respiration with water requires $800 \times 30 = 24{,}000$ times more mass flux through respiratory tissues per unit of extracted oxygen than aerial respiration with all other things being equal. This burden is only slightly eased by the higher extraction efficiency of gills (43).

It has been suggested that the anatomical features of the elpistostegalians—enlarged breathing spiracles at the top of the skull and eyes on top of the skull on bony prominences—enabled stealthy crocodilian-like predatory behavior (8, 13, 40), in which animals are at the surface with their eyes and spiracles just out of the water, looking at the water–land interface for potential prey to attack from the water (*Tiktaalik* in Fig. 5). Possible prey include large terrestrial invertebrates that arrived approximately 50 My before vertebrates (33). Interestingly, one group of these invertebrates, the millipedes, developed chemical defense

systems in the lower Devonian (44). In millipedes that exist today, these systems deter vertebrate predators (45). Hunting in a crocodile-like manner resolves a certain logical tension between the specializations for fully aquatic life seen in the elpistostegalians and adaptations that seem better suited for brief forays onto land: larger eyes and limbs (9, 10) significantly supplemented by tail movement (46).

If air breathing and aerial vision-guided predation of invertebrates on land were early tetrapod adaptations to unfavorable energetics, including low dissolved oxygen within water, it is interesting that the early Carboniferous is also the time when the adelospondyl-colosteid group of digited aquatic tetrapods evolved. Not only did the eyes of this purely aquatic group revert to the mean size of the finned tetrapods (*Greererpeton* in Fig. 2), they also lost their breathing spiracles (8, 47–49), with the possible exemption of some adelospondyls (8, 50). Notably, by this time in the Carboniferous, oxygen levels had more than rebounded from their low in the Devonian (26, 41).

Implications of Long-Range Vision for Reactive Neural Circuits and Planning

Long-range vision has large effects on animal behavior, because it allows more complex decision making over extended sensory ranges. Stimulus-evoked behavior (51) with respect to the most crucial decisions that an organism needs to make, such as an escape response to a looming predator or a lunge at prey, was the normal situation in the aquatic habitats from which land vertebrates originated, where viewing distances were on the order of a body length (*SI Appendix, Reaction Time with Respect to Visual Range in Finned Tetrapods*). With short-range visual stimuli arriving in a just-in-time-to-act fashion, internally driven behavior (52) with serial decision making (53) requiring time proportional to the length of the sequence of actions being deliberated (54) was challenging for actions stemming from perception of dynamic stimuli—such as mobile predators and prey (ref. 55, p. 496). This limitation changed with the evolution of the first long-range (more than 100 body lengths) imaging sensory modality: aerial vision. The only other long-range imaging system in animals is echolocation, which only emerged much later in mammals.

In quite simple instances, an increase in visual range can result in a completely different behavioral control strategy, with large savings in mechanical effort (*SI Appendix, How Temporal/Spatial Range Affects Optimal Decision Making*). After the emergence of vision above the water line, the total volume of space monitored by vision in daylight conditions increased 1 million-fold over that of water in full sunlight, enabling (although not necessitating) complex "deliberative mode" strategies (29, 53, 55) with respect to the most unpredictable features of our environment: other animals. Emergence onto land, with its complex environmental geometry (56) featuring multiple paths toward prey or away from predators, would have furthered the selective benefit of more complex control strategies that take more time to compute than the simplest reactive strategies.

As more behavior became regulated by long-range vision (even with nocturnality) (*SI Appendix*, Table S4), there would have been reduced selective benefit for that portion of the neural infrastructure of the "reactive mode" (29, 55) that aids predator evasion after detection at short range in water. In fish and amphibians, the delay between predator detection and escape is reduced by ≈6 ms (57) through recruiting a single large caliber cell called the Mauthner neuron to initiate the escape maneuver (58). Although this neural circuit enables ultrafast reactions to stimuli (≈4 ms), the limited number of neurons and synapses involved constrains the flexibility of the response (60). Mauthner command cells, activated by close-range acoustic, lateral line, tactile, and looming visual stimuli (59) in proportion to the speed of looming (61), are only present in vertebrates up through amphibians, including frogs (62, 63).

With the evolution of suitable brain circuitry, certain animals were able to consider multiple options for pursuit or evasion that are likely to enhance fitness, such as by vicarious trial and error behavior in rodents, in which future possibilities are imagined (53, 64). Vicarious trial and error, like other forms of prospective cognition or "mental time travel," are dependent on the hippocampus. This structure has the same developmental origin in birds and mammals (65), which had their most recent common ancestor in the Late Carboniferous not long after fully terrestrial animals arose. With this affordance of long-range vision, therefore, we hypothesize that the core neuronal components of planning (53, 65)—now understood to occur in both birds (66) and mammals but less well-studied in reptiles (67)—evolved within a common ancestor (65).

Conclusion

Although the emergence of complete limbs with fingers and toes is central in our imagination of what happened when we transitioned from fish, our results (summarized in Fig. 5) highlight how there was a dramatic change in the information environment of early tetrapods before these anatomical changes occurred. This change in sensory landscape raises the interesting possibility that seeing fitness-enhancing opportunities along the water's edge from afar facilitated the evolution of full terrestriality. We show that eyes nearly tripled in size between when early lobe-finned fish lived and when tetrapods with digited limbs evolved. This big increase in eye size was likely driven by aquatic tetrapods surfacing their eyes above the water line and hunting like crocodiles. This lifestyle caused "primarily aquatic" features to be retained (9, 11, 68), while more and more robust limbs gradually evolved, enabling forays onto land (69). Because small adjustments to optical mechanics evolved to account for the change in the refractive index of air from water, there was an ever-expanding domain of visual awareness, leading these animals to long-range viewing and hunting of the bounty of invertebrate food on the shores. These resources would favor animals evolving morphological adaptations—such as weight-bearing limbs—and neurobehavioral adaptations—such as executing an extended sequence of goal-directed activity—that would enable the exploitation of the new resource. According to the buena vista hypothesis (ref. 55, p. 482), the greatly extended and inexpensive channel of information that long-range vision provided to the opportunities on land may have been central to the evolution of terrestriality and eventually, forms of prospective cognition that this habitat advantages.

Materials and Methods

Selection of Taxa, Phylogenetic Hypothesis, and Time Calibration. Our goal was to select fossils that would cover the initial water to land transition in the Tetrapodomorpha. The habitat preferences of many of the early tetrapods are not exactly known yet, but an increase of terrestriality is generally assumed to have occurred in the Upper Devonian and Early Carboniferous tetrapods. For example, the watcheerid *Pederpes* (Fig. 5) shows foot anatomy that is well-suited for terrestrial locomotion (ref. 8, p. 273), whereas more basal members, such as *Ichthyostega* and *Acanthostega*, are still largely aquatic (8). Hence, we sampled across the stem tetrapod group (sensu Clack). Our selection of taxa was largely guided by prior phylogenies (48, 70–74) to account for phylogenetic covariance. For digited tetrapods, the Early Tetrapod Database (47) was used to identify well-preserved material. To increase the number of well-preserved species, phylogenetic scope was extended crownward to include basal members of the total group Amphibia [Edopoidea and Dendrerpetontidae (74)] and the total group Amniota [Anthracosauria and Gephyrostegidae (72)], which covers most measurable taxa that can be placed in existing phylogenetic hypotheses. Our stemward coverage is less complete, focusing on better known taxa. *Caerorhachis* and *Neopteroplax* were excluded, because their phylogenetic position is unclear. We model the uncertainty caused by poorly

understood phylogenetic relationships for the baphetids, colosteids, and tristichopterids by forming polytomies. We used the stratigraphic ranges of the fossils to time-calibrate the phylogeny with the paleotree package in R (75) (*SI Appendix*, Figs. S1, S2). For the basal tetrapodomorphs, stratigraphic range was based on the dating of the corresponding geological formation extracted from recent papers; for digited tetrapods, the Early Tetrapod Database (47) was used. We used the International Chronostratigraphic Chart (76) to translate to absolute time. Time data were treated as minimum and maximum bounds on single point dates, which were pulled from a uniform distribution. To account for the uncertainty involved in the exact stratigraphic ranges, we repeated this process 1,000 times, resulting in a set of 1,000 time-calibrated phylogenies. The time scaling was performed with the "equal" method, which equally allocates time available on deeper branches to resolve the zero branch length problem (75, 77, 78). Polytomies were resolved randomly for each of the 1,000 trees.

Skull Measurements. Measurements were taken from published drawings and images produced by experts in the field. Eye socket length is defined as the maximum length of the socket, except for in taxa in the digited tetrapod group featuring antorbital vacuities, for which the major axis of an ellipse fit to the orbit alone was used. We define skull length as the distance from the tip of the snout to the caudal margin of the postparietal bones at their medial suture. The extracted measurements are shown in *SI Appendix*, Table S5. Skull source data (images and drawings) used for measurement are in *SI Appendix*.

Defining Eye Size in a Phylogenetic Comparative Framework. We chose the Bayesian implementation of the OU method (5) to assess the adaptive significance of eye socket size differences in early tetrapods. Specifically, we analyzed whether the evolution of relative eye socket size includes changes in the selective regime that may be congruent with periods of change in the water to land transition. This approach does not require prior classification of samples into categories, which is advantageous given that it is currently difficult to assign early tetrapods into discrete habitat categories. Bayesian OU instead agnostically infers whether changes in the selective regime of a trait occurred through evolutionary time and if so, along which branches in the phylogeny these changes likely happened. It is also less prone to error for small phylogenetic comparative datasets ($N < 100$) than other methods (79). We multiplied the traits (i.e., residuals from PGLS) by 10 to avoid computational issues, because the combination of the small-valued residuals and the timespan of more than ≈100 My frequently yielded infinite likelihoods. The analysis was performed over the full set of 1,000 time-calibrated phylogenies using both PGLS with Brownian Motion and OU correlation structure residuals. Probabilistic prior settings were set to package defaults (α, σ^2), but the expected number of shifts in selective regime was set to 12 with an upper limit of 116, the number of branches in the tree. Each branch had the same prior probability to feature a regime shift anywhere along a branch, independent of branch length. The reversible jump Markov chain Monte Carlo simulation was run for 400,000 generations, of which the first 30% was discarded as burn-in. We evaluated the adequacy of the priors by verifying that the estimated parameters were limited to a narrow portion of the entire prior distribution, specifically for the mean (α) and SD (σ^2). To ensure that independent chains had converged on similar regions in the parameter space, we used two approaches: (*i*) Gelman's R for log likelihood, σ^2, and α and (*ii*) a plot of the posterior probabilities for shifts along branches against each other, which should fall along a line with a slope of one if convergence is reached (*SI Appendix*, Fig. S3). A shift in selective regime along a branch was considered well-supported if its respective posterior probability was outside the main distribution of all branches. Four branches with posterior probabilities of 0.15–0.30 (17.4–34.8 times greater than their priors, respectively) were chosen. These four branches consistently featured well-supported shifts across the entire tree set; branches in randomly resolved polytomy regions did not show signatures of selective regime shifts. The choice of type of residuals did not influence the inferred evolutionary pattern of regime shifts. The mean estimate of α is 0.12, indicating a phylogenetic half-life of 5.79 My (6.33 My for OU residuals). These estimates suggest that it took about 12 My to evolve from the ancestral value to the primary adaptive peak, which is congruent with the timespan of the regime shift zone from the first elpistostegalians to the last ancestor of the digited tetrapods (Fig. 2).

Computational Visual Sensory Ecology Estimates. The numerical model for both aquatic and aerial vision contains two components: calculation of the optical stimulus, which can overestimate visual range (particularly in the aerial case), and calculation of the effect of contrast threshold. The framework for calculation of the optical stimulus is adapted from Nilsson et al. (18), which calculates visual range based on the assumption that there are two separate channels that view the background and the target, where channel size is determined by the angular size of the target on the retina (given a particular photoreceptor arrangement) for optimal viewing. A target is said to be visible at a distance if and only if the difference between the photons that arrive from the target and the background are greater than their combined Poisson noise with some reliability coefficient. This relationship can be summarized by the equation:

$$|N_{target} - N_{background}| \geq R\sqrt{N_{target} + N_{background}},$$

where R is the reliability coefficient of 1.96 for 95% confidence, N_{target} is the number of photons detected arriving from the target/object, and $N_{background}$ is the number of photons detected arriving from the background. The number of photons detected due to background illumination and due to space-light between target and viewer is dependent on target width [T (meters)], distance of object [range; r (meters)], the target's apparent radiance [$\hat{R}_O$ (photons meter^{-2} second^{-1} steradian^{-1})], background radiance [$\hat{R}_h$ (photons meter^{-2} second^{-1} steradian^{-1})], dilation or constriction of pupil to adjust for the amount of light [D (meters)], angular size of the target on the retina given that each photoreceptor is distributed on a square array with equal weighting [$(\pi T^2)/(r^2 4)$ (steradian)], and dark noise [false detections; χ (photoisomerizations per rod second^{-1})] (*SI Appendix, Computational Visual Sensory Ecology Estimates*). Based on these dependencies, the numbers of photons detected by the channel viewing only the target and the channel viewing only the background become implicit functions of visual range and pupil diameter. Ranges based on this basic model of firing threshold only account for the physical stimulus that reaches the eye, while neglecting contrast threshold of the eye. This simplification results in overestimating range. To predict the range at which an object becomes invisible, an observer's contrast threshold has to be accounted for (80). Contrast follows the same attenuation law as light [$C_R = C_O e^{-\sigma(\lambda)r}$, where $\sigma(\lambda)$ is the extinction coefficient, C_R is the apparent observed contrast, and C_O is the actual contrast of the object]. If an object's apparent contrast at a given range is smaller than the observer's contrast threshold, the object is said to invisible. Human contrast threshold values as a function of apparent luminance and object angular size were taken from prior work (81). These values were transformed into functions of apparent luminance, angular resolution, and angular size of the object, where angular resolution was chosen to be the diffraction limit, allowing for an implicit pupil diameter and visual range relationship.

The 10-cm black disk size was chosen to be ethologically relevant for the 1- to 2-m body lengths typical of the early tetrapods, but the differences between aquatic and aerial performance reported here are insensitive to size chosen. We estimated the visual sensory volume (18, 29, 82) for this object by a spherical sector of specified radius (from visual range calculations), azimuth, and elevation. For aquatic viewing, we chose an azimuth of 305° [170° per eye minus 35° binocular overlap typical of fish (83)] and an elevation of 60°. For aerial vision, we chose an azimuth of 287° [156° for monocular vision and 25° binocular overlap typical of crocodile (ref. 84, pp. 293–294)] and an elevation of 30°. The aerial vertical field of view of 30° is similar to the vertically compressed field of view provided by the horizontal foveal streak in contemporary crocodile eyes (≈33°) (85), providing a conservative estimate of aerial volume. We do not incorporate the additive effects of eye rotation or head yaw rotation.

Optical Properties of Water for Aquatic Vision Estimates. Because early tetrapods predominantly inhabited freshwater rivers, streams, or estuaries (8, 9, 24–26), light-field simulations were done in waters with higher turbidity and absorption than the clearest ocean water. The Baseline River model (parameter values; *SI Appendix*, Table S3) used in Fig. 4 *A1–D1* was selected, such that the attenuation length at 575 nm was between 0.02 and 2.7 m, the span of values for New Zealand and Alaskan rivers and lakes (22, 23). For example, the Baseline River model's attenuation length of 0.46 m is around the first quartile of lake values and above the median of river values. The water model parameter values were used as input to the radiative transfer program HydroLight (version 5.3; Sequoia Scientific, Inc.) to generate spectral radiance values [$L(z, \theta, \phi, \lambda)$], attenuation coefficient [$c(\lambda) = a(\lambda) + b(\lambda)$], and diffuse attenuation coefficient for radiance in the viewing direction [$K_L(z, \theta, \phi, \lambda)$] for a water column of depth $z = 8$ m. The full moon radiance spectrum (86) was rescaled to give a sea-level irradiance spectrum (that gives a total irradiance in the 400- to 700-nm band of 1×10^{-3} Wm^{-2}), which was inputted into HydroLight. For simulation purposes, it was assumed that the fractional contributions of direct and

diffuse irradiance caused by moonlight and relative angular distribution of the moonlit sky were the same as for a sunlit sky. The resulting photosynthetically available radiation (result of the simulation) was in agreement with experimental results (87). For starlight conditions, an irradiance spectrum provided by Sönke Johnsen, Duke University, Durham, NC, was rescaled to give a total irradiance of 3×10^{-6} W m^{-2}. In HydroLight, starlight was treated as 100% diffuse, because there is no single source.

Sensitivity Analyses. Our selection of three light environments across ±1 SD of finned and digited tetrapod pupil sizes in Fig. 4 itself provides an indication of sensitivity. Additional sensitivity analyses for our selection of water properties were obtained by generating four additional water models that cover a range of intrinsic optical properties and concentration parameters (*SI Appendix*, Table S3). Our findings are not sensitive to these variations (*SI Appendix*, Fig. S6). We also tested more naturalistic contrast values than black, our standard object, which also did not affect our results (*SI Appendix*, Fig. S7). Finally, we tested alternative values for key vision model parameters (*SI Appendix*, Table S2). The new contrast threshold values (K_t) were calculated from relating the human contrast threshold curve (81) to the goldfish contrast threshold (88). The functions relating angular size, contrast threshold, and luminance [$K_t = \Psi(D, T, r, L)$] (definitions are in *SI Appendix*, Table S1) for both goldfish and human were similar enough to be approximated with a shift equal to the mean percentage difference between the two datasets. *SI Appendix*, Table S2 lists the alternative values that were tested. For each parameter, the global extremum (maximum/minimum) of the percentage difference was found and is provided in *SI Appendix*, Table S2. The green fill lower bounds in Fig. 4 are obtained by first selecting a pupil diameter and then finding the minimum value for the corresponding visual performance measure (e.g., range for Fig. 4*A1*) across all alternative values at that pupil diameter. This lower bound estimate is performed for each pupil diameter (1–25 mm). The upper bound is computed similarly but using the maximum value. The vision model sensitivity analysis was only performed for daylight upward viewing within water and daylight viewing in air. Our conclusions are robust to alternative value substitutions. Moreover, given that our alternate values always decrease our nominal underwater metrics (Fig. 4 *A1*–*D1*), it is quite possible that we are overestimating aquatic visual capability. Additional details are provided in *SI Appendix, Sensitivity Analysis*.

ACKNOWLEDGMENTS. We thank Scott Schaper and Olivia Carmo for assistance with data collection and Ian Abraham for coding the ball control example (*SI Appendix*, Fig. S8). We also thank Josef Uyeda for assistance with the bayou package. The image of *Eusthenopteron* is courtesy of John Merck (University of Maryland), and reconstruction of *Acanthostega* is courtesy of Michael Coates (University of Chicago). We thank Sönke Johnsen (Duke University) for providing the starlight spectra used in this study. Marco Gallio, Michael Paulin, and Peter C. Wainwright gave valuable feedback on an earlier draft. This work was partially funded by National Science Foundation Grants IOS-ORG 1456830 (to M.A.M.) and PECASE IOB-0846032 (to M.A.M.), and the support of Northwestern University during M.A.M.'s 3-mo academic leave.

1. Felsenstein J (1985) Phylogenies and the comparative method. *Am Nat* 125(1):1–15.
2. Garland T, Ives AR (2000) Using the past to predict the present: Confidence intervals for regression equations in phylogenetic comparative methods. *Am Nat* 155(3):346–364.
3. Hansen TF (1997) Stabilizing selection and the comparative analysis of adaptation. *Evolution* 51(5):1341–1351.
4. Butler MA, King AA (2004) Phylogenetic comparative analysis: A modeling approach for adaptive evolution. *Am Nat* 164(6):683–695.
5. Uyeda JC, Harmon LJ (2014) A novel Bayesian method for inferring and interpreting the dynamics of adaptive landscapes from phylogenetic comparative data. *Syst Biol* 63(6):902–918.
6. Lu J, et al. (2012) The earliest known stem-tetrapod from the Lower Devonian of China. *Nat Commun* 3:1160.
7. Ruta M, Clack JA (2006) A review of *Silvanerpeton miripedes*, a stem amniote from the Lower Carboniferous of East Kirkton, West Lothian, Scotland. *Trans R Soc Edinb Earth Sci* 97:31–63.
8. Clack JA (2012) Gaining Ground: The Origin and Evolution of Tetrapods (Indiana Univ Press, Bloomington, IN).
9. Daeschler EB, Shubin NH, Jenkins FA (2006) A Devonian tetrapod-like fish and the evolution of the tetrapod body plan. *Nature* 440(7085):757–763.
10. Shubin NH, Daeschler EB, Jenkins FA (2014) Pelvic girdle and fin of Tiktaalik roseae. *Proc Natl Acad Sci USA* 111(3):893–899.
11. Pierce SE, Clack JA, Hutchinson JR (2012) Three-dimensional limb joint mobility in the early tetrapod Ichthyostega. *Nature* 486(7404):523–526.
12. Vorobyeva E, Schultze HP (1991) Description and Systematics of Panderichthyid Fishes with Comments on Their Relationship to Tetrapods (Comstock Publishing Associates, Ithaca, NY), pp 68–109.
13. Long JA, Gordon MS (2004) The greatest step in vertebrate history: A paleobiological review of the fish-tetrapod transition. *Physiol Biochem Zool* 77(5):700–719.
14. Schultze H, Arsenault M (1985) The Panderichthyid fish *Elpistostege*—A close relative of Tetrapods? *Palaeontology* 28(2):293–309.
15. Hall MI (2009) The relationship between the lizard eye and associated bony features: A cautionary note for interpreting fossil activity patterns. *Anat Rec (Hoboken)* 292(6):798–812.
16. Schmitz L (2009) Quantitative estimates of visual performance features in fossil birds. *J Morphol* 270(6):759–773.
17. Angielczyk KD, Schmitz L (2014) Nocturnality in synapsids predates the origin of mammals by over 100 million years. *Proc R Soc B* 281:20141642.
18. Nilsson DE, Warrant E, Johnsen S (2014) Computational visual ecology in the pelagic realm. *Philos Trans R Soc Lond B Biol Sci* 369(1636):20130038.
19. Kirk JTO (1983) Light and Photosynthesis in Aquatic Ecosystems (Cambridge Univ Press, Cambridge, UK).
20. Mobley CD (1995) The optical properties of water. Handbook of Optics, ed Bass M (McGraw-Hill, New York), 2nd Ed Vol 1, pp 43.3–43.56.
21. Davies-Colley RJ, Nagels JW (2008) Predicting light penetration into river waters. *J Geophys Res Biogeosci* 113(G3):1–9.
22. Davies-Colley RJ (1988) Measuring water clarity with a black disk. *Limnol Oceanogr* 33(4):616–623.
23. Koenings J, Edmundson J (1991) Secchi disk and photometer estimates of light regimes in Alaskan lakes: Effects of yellow color and turbidity. *Limnol Oceanogr* 36(1):91–105.
24. Narkiewicz M, et al. (2015) Palaeoenvironments of the Eifelian dolomites with earliest tetrapod trackways (Holy Cross Mountains, Poland). *Palaeogeogr Palaeoclimatol Palaeoecol* 420:173–192.
25. Retallack GJ (2011) Woodland hypothesis for Devonian tetrapod evolution. *J Geol* 119(3):235–258.
26. Clack JA (2007) Devonian climate change, breathing, and the origin of the tetrapod stem group. *Integr Comp Biol* 47(4):510–523.
27. Killinger D, Churnside J, Rothman L (1995) Atmospheric optics. Handbook of Optics, ed Bass M (McGraw-Hill, New York), 2nd Ed Vol 1, pp 44.1–44.49.
28. Middleton WEK (1952) Vision Through the Atmosphere (Univ of Toronto Press, Toronto).
29. Snyder JB, Nelson ME, Burdick JW, MacIver MA (2007) Omnidirectional sensory and motor volumes in an electric fish. *PLoS Biol* 5(11):2671–2683.
30. MacIver MA, Shirgaonkar AA, Patankar NA (2010) Energy-information trade-offs between movement and sensing. *PLoS Comput Biol* 6(5):e1000769.
31. Cronin TW, Johnsen S, Marshall NJ, Warrant EJ (2014) Visual Ecology (Princeton Univ Press, Princeton).
32. Mobley C, Boss E, Roesier C (2016) *Ocean Optics, Light and Radiometry, Visualizing Radiances*. Available at www.oceanopticsbook.info. Accessed September 17, 2016.
33. Shear WA, Edgecombe GD (2010) The geological record and phylogeny of the Myriapoda. *Arthropod Struct Dev* 39(2-3):174–190.
34. Nilsson DE, Pelger S (1994) A pessimistic estimate of the time required for an eye to evolve. *Proc Biol Sci* 256(1345):53–58.
35. Nilsson DE, Warrant EJ, Johnsen S, Hanlon R, Shashar N (2012) A unique advantage for giant eyes in giant squid. *Curr Biol* 22(8):683–688.
36. Laughlin SB (2001) Energy as a constraint on the coding and processing of sensory information. *Curr Opin Neurobiol* 11(4):475–480.
37. Niven JE, Laughlin SB (2008) Energy limitation as a selective pressure on the evolution of sensory systems. *J Exp Biol* 211(11):1792–1804.
38. Moran D, Softley R, Warrant EJ (2015) The energetic cost of vision and the evolution of eyeless Mexican cavefish. *Sci Adv* 1(8):e1500363.
39. Lewis JE, Gilmour KM, Moorhead MJ, Perry SF, Markham MR (2014) Action potential energetics at the organismal level reveal a trade-off in efficiency at high firing rates. *J Neurosci* 34(1):197–201.
40. Graham JB, et al. (2014) Spiracular air breathing in polypterid fishes and its implications for aerial respiration in stem tetrapods. *Nat Commun* 5:3022.
41. Royer DL, Donnadieu Y, Park J, Kowalczyk J, Goddéris Y (2014) Error analysis of CO_2 and O_2 estimates from the long-term geochemical model GEOCARBSULF. *Am J Sci* 314(9):1259–1283.
42. Glass ML, Rantin FT (2009) Gas Exchange and Control of Respiration in Air-Breathing Teleost Fish, eds Glass LM, Wood CS (Springer, Berlin), pp 99–119.
43. Glass ML (2009) Physiological Evidence Indicates Lungfish as a Sister Group to the Land Vertebrates, eds Glass LM, Wood CS (Springer, Berlin), pp 161–177.
44. Wilson HM (2006) Juliformian millipedes from the lower Devonian of Euramerica: Implications for the timing of millipede cladogenesis in the Paleozoic. *J Paleontol* 80(4):638–649.
45. Shear WA (2015) The chemical defenses of millipedes (diplopoda): Biochemistry, physiology and ecology. *Biochem Syst Ecol* 61:78–117.
46. McInroe B, et al. (2016) Tail use improves performance on soft substrates in models of early vertebrate land locomotors. *Science* 353(6295):154–158.
47. Benton MJ, Ruta M, Dunhill AM, Sakamoto M (2013) The first half of tetrapod evolution, sampling proxies, and fossil record quality. *Palaeogeogr Palaeoclimatol Palaeoecol* 372:18–41.
48. Bolt JR, Lombard RE (2010) *Deltaherpeton hiemstrae*, a new colosteid tetrapod from the Mississippian of Iowa. *J Paleontol* 84(6):1135–1151.
49. Carroll R (1969) A new family of Carboniferous amphibians. *Palaeontology* 12(4):537–548.

50. Carroll RL (1967) An adelogyrinid lepospondyl amphibian from the Upper Carboniferous. *Can J Zool* 45(1):1–16.
51. Jun JJ, Longtin A, Maler L (2014) Enhanced sensory sampling precedes self-initiated locomotion in an electric fish. *J Exp Biol* 217(20):3615–3628.
52. Haggard P (2008) Human volition: Towards a neuroscience of will. *Nat Rev Neurosci* 9(12):934–946.
53. Redish AD (2016) Vicarious trial and error. *Nat Rev Neurosci* 17(3):147–159.
54. Rosenbaum DA, Cohen RG, Jax SA, Weiss DJ, van der Wel R (2007) The problem of serial order in behavior: Lashley's legacy. *Hum Mov Sci* 26(4):525–554.
55. MacIver MA (2009) Neuroethology: From morphological computation to planning. The Cambridge Handbook of Situated Cognition, eds Robbins P, Aydede M (Cambridge Univ Press, New York), pp 480–504.
56. Stein WE, Berry CM, Hernick LV, Mannolini F (2012) Surprisingly complex community discovered in the mid-Devonian fossil forest at Gilboa. *Nature* 483(7387):78–81.
57. Kohashi T, Oda Y (2008) Initiation of Mauthner- or non-Mauthner-mediated fast escape evoked by different modes of sensory input. *J Neurosci* 28(42):10641–10653.
58. Zottoli SJ, Faber DS (2000) The Mauthner cell: What has it taught us? *Neuroscientist* 6(1):26–38.
59. Preuss T, Osei-Bonsu PE, Weiss SA, Wang C, Faber DS (2006) Neural representation of object approach in a decision-making motor circuit. *J Neurosci* 26(13):3454–3464.
60. Catania KC (2009) Tentacled snakes turn C-starts to their advantage and predict future prey behavior. *Proc Natl Acad Sci USA* 106(27):11183–11187.
61. Bhattacharyya KD, McLean D, MacIver MA (2016) Trade-offs between speed and variability in responses to looming visual stimuli. Proceedings of the 46th Annual Meeting of the Society for Neuroscience (SfN) (San Diego).
62. Bierman HS, Zottoli SJ, Hale ME (2009) Evolution of the Mauthner axon cap. *Brain Behav Evol* 73(3):174–187.
63. Will U (1991) Amphibian Mauthner cells. *Brain Behav Evol* 37(5):317–332.
64. Tolman E (1939) Prediction of vicarious trial and error by means of the schematic sowbug. *Psychol Rev* 46(4):318–336.
65. Allen TA, Fortin NJ (2013) The evolution of episodic memory. *Proc Natl Acad Sci USA* 110:10379–10386.
66. Clayton NS, Emery NJ (2015) Avian models for human cognitive neuroscience: A proposal. *Neuron* 86(6):1330–1342.
67. Wilkinson A, Huber L (2012) Cold-blooded cognition: Reptilian cognitive abilities. Oxford Handbook of Comparative Evolutionary Psychology, eds Vonk J, Shackleford K (Oxford Univ Press, Oxford).
68. Coates M (1996) The Devonian tetrapod *Acanthostega gunnari* Jarvik: Postcranial anatomy, basal tetrapod interrelationships and patterns of skeletal evolution. *Trans R Soc Edinb Earth Sci* 87(3):363–421.
69. Gunter G (1956) Origin of the tetrapod limb. *Science* 123(3195):495–496.
70. Swartz B (2012) A marine stem-tetrapod from the Devonian of western North America. *PLoS One* 7(3):e33683.
71. Anderson PSL, Friedman M, Ruta M (2013) Late to the table: Diversification of tetrapod mandibular biomechanics lagged behind the evolution of terrestriality. *Integr Comp Biol* 53(2):197–208.
72. Ruta M, Coates MI (2007) Dates, nodes and character conflict: Addressing the lissamphibian origin problem. *J Syst Palaeontol* 5(1):69–122.
73. Milner AC, Milner AR, Walsh SA (2009) A new specimen of *Baphetes* from Nýřany, Czech Republic and the intrinsic relationships of the Baphetidae. *Acta Zool* 90(Suppl 1):318–334.
74. Schoch RR (2013) The evolution of major temnospondyl clades: An inclusive phylogenetic analysis. *J Syst Palaeontol* 11(6):673–705.
75. Bapst DW (2012) paleotree: An R package for paleontological and phylogenetic analyses of evolution. *Methods Ecol Evol* 3(5):803–807.
76. Cohen KM, Finney SC, Gibbard PL, Fan JX (2013) The ICS International Chronostratigraphic Chart, update v2015/01. *Episodes* 36(3):199–204.
77. Brusatte SL, Benton MJ, Ruta M, Lloyd GT (2008) Superiority, competition, and opportunism in the evolutionary radiation of dinosaurs. *Science* 321(5895):1485–1488.
78. Lloyd GT, Wang SC, Brusatte SL (2012) Identifying heterogeneity in rates of morphological evolution: Discrete character change in the evolution of lungfish (Sarcopterygii; Dipnoi). *Evolution* 66(2):330–348.
79. Cooper N, Thomas GH, Venditti C, Meade A, Freckleton RP (2016) A cautionary note on the use of Ornstein Uhlenbeck models in macroevolutionary studies. *Biol J Linn Soc Lond* 118(1):64–77.
80. Duntley SQ (1948) The visibility of distant objects. *J Opt Soc Am* 38(3):237–249.
81. Blackwell HR (1946) Contrast thresholds of the human eye. *J Opt Soc Am* 36(11):624–643.
82. Nelson ME, MacIver MA (2006) Sensory acquisition in active sensing systems. *J Comp Physiol A* 192(6):573–586.
83. Land MF, Nilsson DE (2012) Animal Eyes, Oxford Animal Biology Series (Oxford Univ Press, Oxford), 2nd Ed.
84. Walls GL (1963) The Vertebrate Eye and Its Adaptive Radiation (Hafner Publishing Company, New York), 2nd Ed.
85. Nagloo N, Collin SP, Hemmi JM, Hart NS (2016) Spatial resolving power and spectral sensitivity of the saltwater crocodile, *Crocodylus porosus*, and the freshwater crocodile, Crocodylus johnstoni. *J Exp Biol* 219(9):1394–1404.
86. Steen M (2014) *Spectrum of Moonlight*. Available at www.olino.org/us/articles/2015/10/05/spectrum-of-moon-light. Accessed July 11, 2016.
87. Raven J, Cockell C (2006) Influence on photosynthesis of starlight, moonlight, planetlight, and light pollution (reflections on photosynthetically active radiation in the universe). *Astrobiology* 6(4):668–675.
88. Hester FJ (1968) Visual contrast thresholds of goldfish (*Carassius auratus*). *Vision Res* 8(10):1315–1335.